

INDOOR AIR NO₂ DEPOLLUTION BY PHOTOCATALYSIS – COMPARING REACTOR AND EXPERIMENTAL CHAMBER RESULTS

JIVKO TOPALOV¹, JULIE HOT¹, ERICK RINGOT^{1,2} & ALEXANDRA BERTRON¹

¹LMDC, Université de Toulouse, INSA/UPS Génie Civil, France

²LRVision SARL, ZI de Vic, France

ABSTRACT

Air quality improvement is a major concern in developed countries. In the past decade, especially in Europe, legislative measures have been taken to reduce air pollution. The present article promotes photocatalysis as an air quality improvement technique towards NO₂ pollution. Indoor air depollution by painted plasterboards treated with photocatalytic coating was investigated. First, at laboratory scale, using a bed flow reactor, depollution efficiency of the photocatalytic system was evaluated. Experimental conditions were adapted as much as possible to match indoor environment. Thus, pollution levels remained at ppb scale, temperature and relative humidity (RH) were kept constant (20 °C and 50% RH) and typical indoor lighting systems (fluorescent tubes, Light-Emitting Diode (LED) and halogen bulbs) were used for photoactivation. UV-A fluorescent tube was also used to optimise photocatalytic activity. Second, experiments were conducted at real scale, in a 10-m³ experimental chamber developed at our laboratory. Interior walls were covered with the photocatalytic system and the chamber was used as a reactor. Employing a specific experimental procedure, aiming at keeping pollution level constant in the chamber, photocatalytic depollution was evaluated. The same lighting systems were used for photoactivation. NO₂ abatement efficiency was evaluated through the photocatalytic oxidation potential and rate. Results show that NO₂ can be significantly removed by this technique. However, the light used for photoactivation is at utmost importance. Furthermore, the results show that at laboratory scale, photocatalytic depollution efficiency of NO₂ could be underestimated.

Keywords: depollution, experimental chamber, indoor air quality, in situ, photocatalysis, TiO₂, NO₂, UV-A light, visible light

1 INTRODUCTION

Over the past two decades, photocatalysis (mainly based on TiO₂ semiconductor) has been widely studied as an air depollution technique regarding NO_x [1–8] under real scale configuration. Depollution tests were performed in an artificially closed area of the parking, which was polluted by a car exhaust during the testing period. The ceiling surface of the car park was covered with white acrylic TiO₂-containing paint (PP). However, studies differ by the experimental setup used and the experimental conditions employed. This renders comparison of experimental results ambiguous; some authors find photocatalysis has a strong potential towards NO_x depollution [9–12] like nitric oxide (NO), while others state that this technique is ineffective [13, 14] for nitrogen dioxide (NO₂). This shows that there is a necessity, not only in standardising laboratory setups and experimental procedures, but also in conducting innovative in situ experiments. As a matter of fact, recommendations and international standards for laboratory experiments already exist [15] but are not always followed. Moreover, some authors criticise them and state they must be reevaluated [16]. Furthermore, actual standards are not adapted to indoor environment conditions, such as ppb pollution level and light wavelengths and intensities used.

Regarding in situ applications, studies can be found in literature [2, 10, 14, 17–19] but only a handful of them are regarding indoor applications.

In this article, photocatalytic efficiency of painted plasterboards treated with a TiO_2 -based coating was evaluated towards indoor air applications. First, in laboratory conditions (bed flow reactor) and then in “real-world” conditions (a-10 m^3 experimental chamber). The purpose was to show that photocatalysis could be used to enhance indoor air quality regarding NO_x . Thus, all experiments were conducted under conditions representative of indoor environments – ppb level of pollution, typical indoor light, ambient temperature (23 °C) and relative humidity (RH) (50%).

2 MATERIALS AND METHODS

2.1 Photocatalytic material

The photocatalytic material in this study consisted of orange-painted plasterboards (used as substrate) coated with a TiO_2 anatase aqueous solution (used as photocatalyst). First, standard plasterboards (Placoplatre® BA 13) were purchased. Each plasterboard was then cut into pieces with specific dimensions fitting the reactor or the experimental chamber. For the bed flow reactor, three pieces were prepared respecting the normalised dimensions 10×5 cm^2 . For the experimental chamber, a total of 28 pieces were prepared. Four sizes were used in order to fit on the indoor walls (100×50 cm^2 , 75× cm^2 , 50×50 cm^2 and 50×25 cm^2). For each piece, edge bands were covered with an adhesive tape in order to limit adsorption. Each plasterboard plate was then painted with orange water-based acrylic paint containing natural pigment (provided by LRVision Company). Two layers were applied using a paint roller and a brush.

The photocatalytic dispersion was prepared by diluting a water-based commercial product (CristalACTiV™ S5-300B, TiO_2 anatase content: 18 wt%) to obtain an aqueous solution containing 6 wt% of dry matter TiO_2 . Dispersion was then applied to plasterboard surfaces with the help of a brush. The total quantity of TiO_2 (dry matter) on substrate surfaces was $2.9 \pm 0.1 \text{ g/m}^2$ for the experimental chamber plates and $3.1 \pm 0.1 \text{ g/m}^2$ for the reactor samples. This quantity was controlled by weighing the recipient containing the TiO_2 dispersion before and after coating each plasterboard sample. The targeted value of 3 g/m^2 of photocatalytic product on surface was chosen according to previous research work carried out by the same authors [20]. Finally, each reactor sample was tested separately, while the 28 plasterboards plates (a total surface of 9.3 m^2) were all mounted on the walls inside the experimental chamber, covering about half of the total indoor surface (ceiling, floor, door and window excluded).

2.2 Laboratory setup

Under laboratory conditions, NO_2 depollution efficiency of our photocatalytic materials was investigated using a specific experimental setup inspired from ISO 22197-1 [15]. A detail description can be found in previous work [20]. Here, a schematic representation is given in Fig. 1 and the setup is briefly described.

A borosilicate-glass reactor (free volume of about 400 cm^3) with a cylindrical shape was used. Polluted air (100 ppb of NO_2) was dynamically introduced in the reactor with a constant flow rate of 1.5 ln/min . This was achieved by diluting NO_2 stream (gas bottle Air Liquide 8 ppb) with two air streams (zero air generator Environment SA ZAG7001). Each stream was adjusted by mass flow controllers (MFCs) (Bronkhorst EI-Flow Select). One of the air

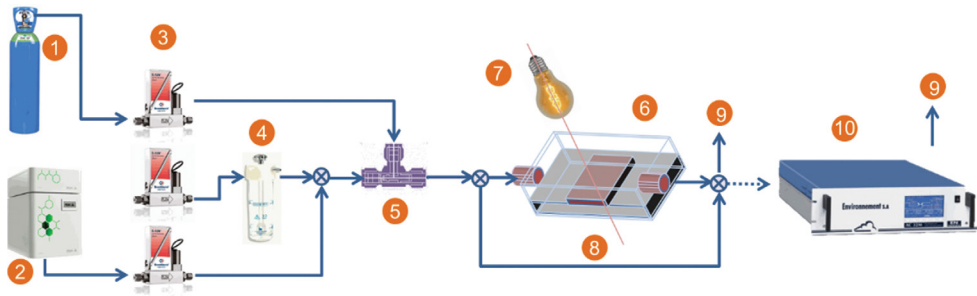


Figure 1: Schematic diagram of the experimental setup for NO₂ degradation. (1) NO₂ gas cylinder (8 ppm), (2) zero-air generator, (3) mMFCs, (4) washing bottle, (5) mixing chamber, (6) borosilicate-glass reactor with temperature and humidity probe, (7) lighting system, (8) bypass, (9) extraction system, (10) NO_x analyser.

streams was dried and the other humidified using a washing bottle, which controlled the humidity level. A chemiluminescent NO_x analyser (Environment SA AC32M) sampled polluted air exiting the reactor. Finally, the temperature and RH inside the reactor were measured with a probe (KIMO).

2.3 Experimental house

Under “real-world” conditions, NO₂ depollution efficiency of our photocatalytic materials was investigated using a small experimental house designed by the LMDC (Laboratory of Materials and Durability of Constructions, UPS/INSA, Toulouse, France). This house was used in previous works [18, 19]. A schematic representation and pictures of this experimental house are shown in Fig. 2.

The isolated house divided the house into two chambers: (1) the experimental chamber and (2) the control chamber, connected only by two stainless tubes ($\varphi=6$ mm) through the internal wall. One was used for gaseous pollutant injection, the other for air sampling.

With a volume of roughly 10 m³, the experimental chamber was used as a vast photocatalytic reactor and an air fan was installed for ensuring pollution homogenisation and test repeatability. Gaseous pollution was injected inside from the control chamber and was then diluted in the indoor air. A part of this air was sampled. Due to natural leakage, indoor/outdoor exchanges occurred so a standardised air tightness test was conducted [21]. The obtained result with an overpressure/undrpressure of 4 Pa ($Q_{4\text{Pa-surfi}}$) was 1.32–1.44 m³.h⁻¹.m⁻². Therefore, the chamber was qualified as class D. However, this indicator is not suitable for quantifying pollution leakage.

The purpose of this chamber was to assess photocatalytic activity occurring on the walls. Rather than treating directly existing interior wall surfaces, the photocatalyst was applied to removable plasterboards covering the walls. This enables various photocatalytic materials to be tested. On the chamber ceiling, artificial lighting systems were installed to test various illumination conditions. All tests were carried out, while shutters were closed. This ensured no interference with natural light and allowed tests to be carried out without activating the photocatalytic material. Temperature, RH and indoor/outdoor pressure variations were not controlled but were constantly measured by probes (KIMO). Moreover, during tests, the

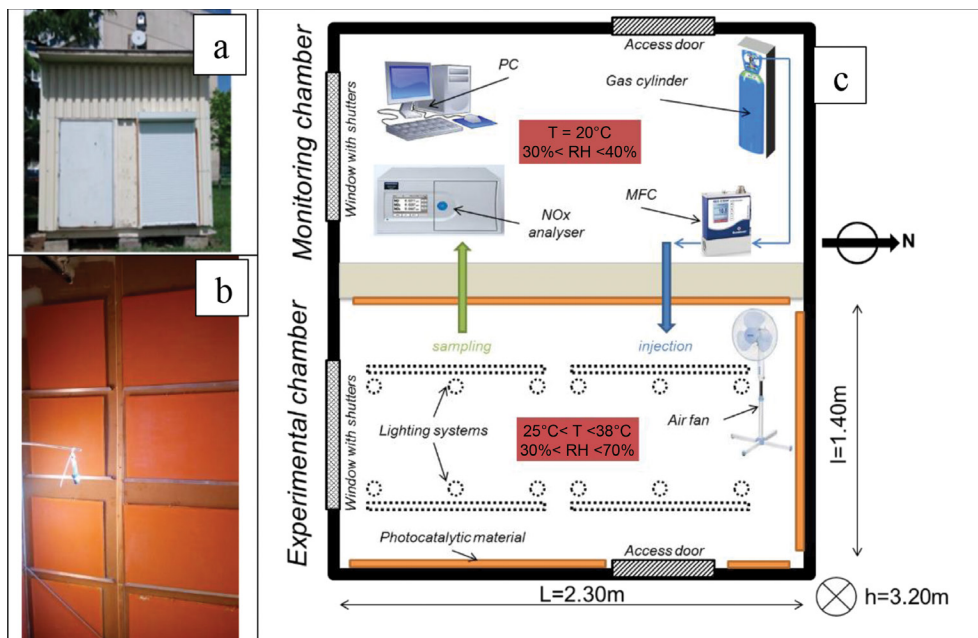


Figure 2: Experimental house developed at the LMDC for photocatalytic assessment – (a) picture of outside view (South wall), (b) picture of the photocatalytic material (North wall), (c) inside schematic representation (top view).

interior of the experimental chamber could be observed in the monitoring chamber via a camera.

The monitoring chamber was used to govern experiments. As it can be seen in Fig. 2c, a gas cylinder (Air Liquide – 45 ppm of NO_2 stabilised in N_2) connected to a MFC (from M+W Instrumentation) enabled pollution flow rate control before injection in the experimental chamber through the first stainless tube. Using the second stainless tube, polluted air was sampled at 1 l/min without affecting the pollution level inside the experimental chamber. A NO_x analyser (HORIBA APNA-370) was used to measure NO_x (NO and NO_2) concentrations in the sampled air. This apparatus gave instantaneous results and allowed a continuous monitoring and recording (one mean value each 5 min). To preserve equipment service life, temperature and RH were controlled by air conditioning (20°C and 30-40% RH). Finally, artificial lighting was also switched on/off from this room.

2.4 Lighting conditions

Photocatalysis activity is governed by light wavelengths and intensities. As shown in literature, UV-A light with wavelengths ranging from 370 to 380 nm are well adapted for TiO_2 activation [4, 22–24]. However, these wavelengths are very limited indoors, and thus photocatalytic efficiency in these environments could be debatable. In order to clarify this problem, in this article, experiments were carried out under typical indoor lighting conditions. Three different visible light lamps were used: (1) fluorescent tubes (Sylvania Luxline T8, 30 W,

2400 lm), (2) Light-Emitting Diode (LED) bulbs (GE Energy Smart, 40 W, 470 lm) and (3) halogen bulbs (Lumipro Eco, 55 W, 630 lm). Experiments were also conducted under UV light provided by fluorescent tubes (Narva Blacklight blue LT-T8, 30 W) to get results under optimal conditions. Thus, at both scales (reactor and chamber), lighting conditions were characterised by the type of lamp, its wavelength and the irradiation intensity received on the photocatalytic surfaces. Light intensity was measured with a radiometer (Gigahertz-Optik X1.1 Optometer) equipped with two detectors: UV-A detector for wavelength between 315 and 400 nm (model UV-3717) and visible detector for wavelengths between 400 and 800 nm (model RW-3703). Moreover, a previous measurement campaign was carried out at the LMDC, and three rooms were targeted (office, laboratory room and classroom) in order to get an idea on a typical indoor light magnitude. For more details, see [20]. This allowed us to conclude that in all cases, experimental lighting conditions tested were considered as being representative of indoor environments.

First, light intensity received by the photocatalytic material surface was investigated. At reactor scale, the photocatalytic surface was equally irradiated since the light source was directly above the sample. Results are given in Table 1. This was not the case in the chamber since each plate was located at a different distance from the light source. Around 100 selected points allowed mapping light intensity distribution on the walls. Detailed results can be found in our previous work [19]. Here, each lighting condition was expressed by the mean intensity value obtained at three different heights. The results are summarised in Table 1. Finally, visible wavelengths under UV light and UV wavelengths under visible light were negligible.

Second, spectrum emission on each light was investigated. According to the UV-A lamp data sheet, distribution spectrum varies between 350 and 400 nm with a peak around 365 nm. In the case of visible lighting, emission wavelengths have been investigated using a spectroradiometer (Jeti specbos 1201) and distribution spectrum of each lamp was obtained between 380 and 780 nm. Results are given in Fig. 3. Fluorescent lamp showed a discontinuous spectrum: luminous intensity was focused on three major peaks – 436 nm, 544 nm and 612 nm. Halogen lamp had a rising continuous spectrum with no dominant wavelengths. LED lamp had a first peak around 450 nm and a second one around 605 nm, which were wider than the peaks of fluorescent light.

Table 1: Mean light irradiation values received by the photocatalytic material in the reactor and the experimental chamber (in mW/m²).

Height (cm)	Reactor			
	UV lighting 315< λ <400 nm		Visible lighting 400< λ <800 nm	
15	Fluorescent	Fluorescent	Halogen	LED
	950 ± 50	6200 ± 100	5800 ± 100	5900 ± 100
	Chamber			
20	40 ± 20	400 ± 100	900 ± 100	300 ± 100
100	300 ± 50	1000 ± 200	1700 ± 300	800 ± 200
180	1200 ± 300	2500 ± 500	6100 ± 500	2300 ± 300

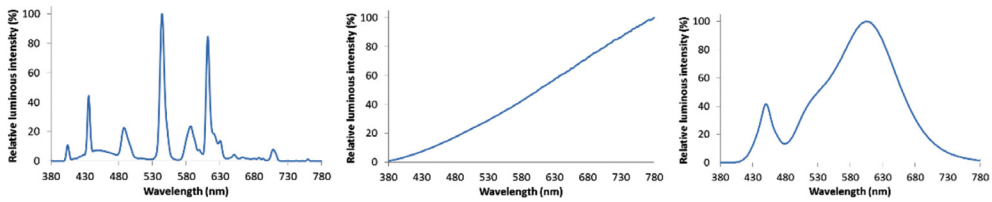


Figure 3: Spectrum distribution between 380 and 780 nm: (a) fluorescent, (b) halogen, (c) LED.

2.5 Experimental procedure

2.5.1 Laboratory scale

The experimental procedure was inspired by ISO 22197-1 [15] and adapted to NO_2 . The first step was carried out in the dark and ensured that exiting pollution is 100 ppb of NO_2 . Since tests were carried out under continuous injection, the pollution level was constant. Total flow rate (pollution, dry air and humidified air) was fixed at 1.5 Ln/min, RH was measured around 50 % and temperature was around 23°C. Approximately 30–45 min was required to ensure concentration stability before tests could be performed. Each experiment lasted 100 min. During the first 20 min, concentration was monitored in the dark. During the following 60 min, samples were irradiated by visible light (20 min per light type; LED, halogen and fluorescent). Over the last 20 min, samples were irradiated by UV-A light. For each irradiation conditions, NO_2 depollution was measured and efficiency was calculated with respect to pollution level measured under dark. Typical evolution of NO and NO_2 during a test is illustrated in Fig. 4.

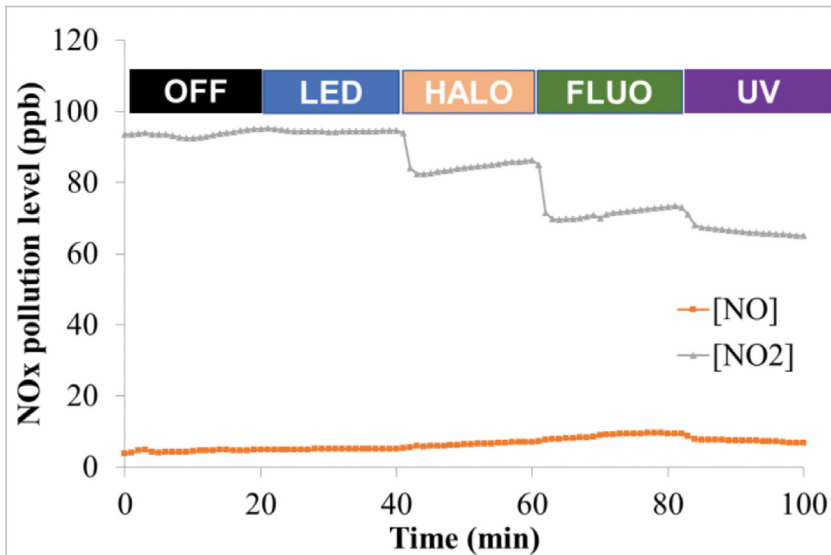


Figure 4: Typical evolution of NO_x (i.e. NO and NO_2) pollution levels exiting the reactor during a 100-min test.

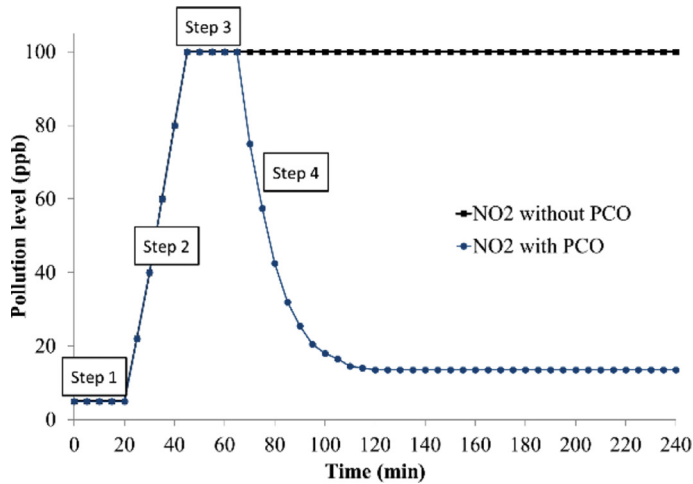


Figure 5: A theoretical step by step diagram of the experimental procedure followed.

2.5.2 In situ scale

Photocatalytic efficiency under “real-world” conditions was investigated under dynamic NO_2 injection. Experimental procedure consisted of polluting the chamber to a certain level (here 100 ppb of NO_2), then maintaining pollution level before activating the photocatalytic material. The procedure was also used to evaluate NO efficiency in previous work [19]. The four steps illustrated in Fig. 5 summarise the procedure:

- **Step 1:** Background NO_x level assessment: no pollution injection, 20 min.
- **Step 2:** Reaching 100 ppb of NO_2 : 1.5 Ln/min of NO_2 injection, 25 min
- **Step 3:** Maintaining 100 ppb of NO_2 : 0.78 ± 0.05 Ln/min of NO_2 injection, 200 min
- **Step 4:** Photocatalytic activation: after observing pollution stability for 20 min, lights are switched ON, 180 min

3 RESULTS AND DISCUSSIONS

3.1 Photocatalytic degradation in laboratory

At laboratory scale, the photocatalytic depollution capabilities of three samples were investigated. Results averaged for the three samples are given in Table 2. We remind readers that those experiments are conducted in order to get an idea of the efficiency at this scale, then compare results with those obtained at chamber scale.

First, the average concentration during dark is 95 ppb, while 100 ppb has been injected (measured while reactor does not contain sample). This is due to adsorption of NO_2 on the material surface [5, 25, 26]. In order to measure pollution variation due only to photocatalytic degradation, we ensured that maximum adsorption was reached (i.e. no concentration variation during dark) before turning light ON. This was achieved by pre-exposing each sample for about 30–45 min to polluted air in the reactor under dark. Under LED light, there seems to be no photocatalytic activity. This is mostly due to the fact that LED used in this study

Table 2: Results obtained at reactor scale for all irradiation. $[X]_{out}$ (ppb) is the average concentration at the reactor exit, ξ (%) is the average photocatalytic efficiency.

NO₂ outlet concentration ($[X]_{out}$ in ppb) and photocatalytic efficiency (ξ in %)										
Light OFF		LED		Halogen		Fluorescent		UV-A		
$[X]_{out}$	ξ	$[X]_{out}$	ξ	$[X]_{out}$	ξ	$[X]_{out}$	ξ	$[X]_{out}$	ξ	
NO ₂	95	-	95	0	84	10	71	27	66	36

did not emit sufficiently short wavelengths capable of activating the photocatalytic surface. As illustrated in Fig. 3c, emission starts around 410 nm. Under halogen light, pollution is reduced and the photocatalytic efficiency was around 10%. Under fluorescent visible light pollution was further reduced and efficiency was around 27%. Both light emits wavelengths shorter than 410 nm. This confirms our hypothesis that our photocatalytic material requires shorter wavelengths to be activated. Finally, under UV-A, pollution is furthermore reduced and efficiency was estimated around 36%. This shows that indeed UV-A is the optimal light for photocatalytic depollution. Nevertheless, using visible light emitting wavelengths under 410 nm decent depollution results could be obtained.

One should have in mind that efficiency obtained here could be boosted to up to 50% if more TiO₂ is deployed to the surface [20]. However, this is not our objective since we wanted to compare the results with those obtained at chamber scale where photocatalyst is deployed at same level.

3.2 Photocatalytic degradation in experimental chamber

3.2.1 Importance of light

Experimental results in the chamber for all light types used in our study are shown in Fig. 6. First, while lights are OFF, pollution level was maintained constant over 200 min with slight variations. This confirms that experimental procedure allowed neutralising leakage and keeping pollution level constant. Second, results seem to be in agreement with those obtained in the reactor. Under LED, no degradation was observed. This confirms that this type of light was not appropriate for our photocatalytic material. However, in some cases where TiO₂ is doped to adsorb wavelengths in the visible area [27, 28] this light could possibly show interesting results. Under fluorescent and halogen light, degradation appears similar. As can be observed, after 60 min of irradiation, photocatalysis reaches its maximum potential. Pollution was reduced to about 50 ppb and was maintained at this level even though injection continued. Results differed from those obtained on a reactor, where halogen had a lesser efficiency, but here irradiation produced by this light was stronger (see Table 1). Finally, under UV-A, highest degradation was observed. After 45 min, maximum photocatalytic potential was achieved and pollution level was reduced to 20 ppb.

3.2.2 Photocatalytic efficiency

Results obtained in the experimental chamber were investigated using two methods. Those were also used in our previous study [19] regarding NO. Since it is an in situ experiment, no standards and recommendations exist for the photocatalytic depollution estimation.

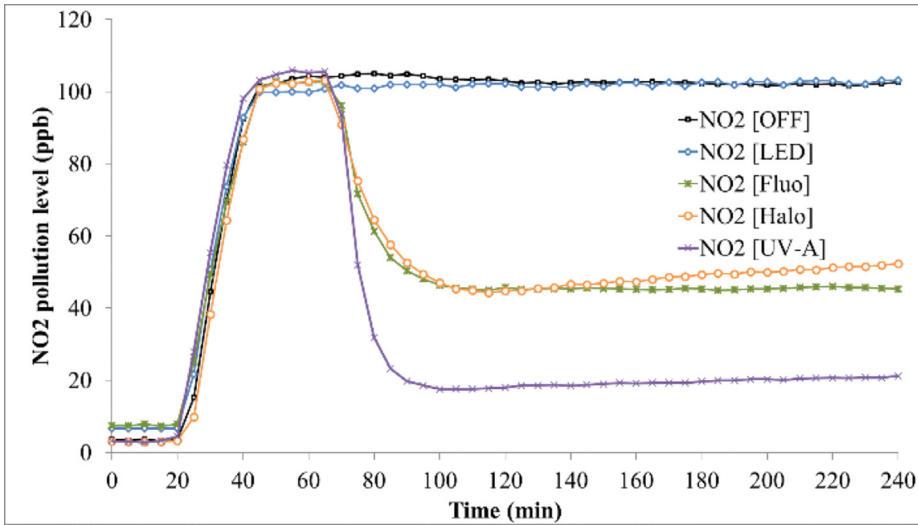


Figure 6: NO₂ photocatalytic degradation in the experimental chamber under various lighting systems – OFF, LED, fluorescent, halogen and UV-A.

The first method evaluates efficiency throughout the slope and the lowest NO₂ level measured while light was active and gas was still injected. Results are summarised in Table 3. We observed that both parameters are related; the higher the slope, the lower the NO₂ level.

The second method evaluates efficiency throughout the mass of NO₂ destroyed. Since we controlled injection and we continuously measured NO₂ levels in the chamber, we could calculate the mass of NO₂ destroyed per unit of time. Also, knowing the total surface of the photocatalytic material, we could estimate the depollution effect per square meter and thus give some durable criteria for the photocatalytic efficiency. Results are presented in Table 4 and show that depollution rate under UV was near 3.5 µg/min⁻¹/m⁻² and around 2 µg/min⁻¹/m⁻² under visible light.

Table 3: PCO potential: slope and lowest NO₂ level for all lighting systems used.

Slope and lowest NO ₂ level	Light			
	UV-A	Fluorescent	Halogen	LED
Slope (ppb/min)	4.7	2.9	2.6	0
Min NO ₂ (ppb)	20	48	48	100

Table 4: PCO degradation rate for all lighting systems used.

PCO degradation rate	Light			
	UV-A	Fluorescent	Halogen	LED
Mass of NO ₂ destroyed (µg/min ⁻¹ /m ⁻²)	3.47	2.23	1.94	0

3.3 Comparing reactor and experimental chamber efficiency

Due to the large difference between the two scales (volume, surface, volume to surface or surface to volume ratio, pollution residence time, contact between surface and pollutant, presence of other pollutants, etc.), correlating reactor and chamber results was a tricky task. However, using the same photocatalytic material and the same illuminating conditions, some conclusions can be drawn. First, reactor and chamber depollution follows similar trends. Under UV-A light, in both scales, best degradation results were obtained. Regarding visible light, in both scales, LED showed no photo activity. This shows that reactors can be used to investigate the photo activity. If no activity is detected at reactor scale, no activity will also be detected at a larger scale if irradiation conditions are alike. It should be noted that under similar intensities (6.2 W/m² for fluorescent vs 5.8 W/m² for halogen) fluorescent light seems more adapted to the photo activity at this scale. (6.2 W/m² for fluorescent vs 5.8 W/m² for halogen). This was confirmed at the chamber where depollution seemed equal; however fluorescent light produced weaker intensity (2.5 W/m² vs 6.1 W/m² at 180 cm from ground floor). If fluorescent light was stronger, depollution should be higher. In any case, halogen irradiation was similar at the reactor and the chamber. Despite that, efficiency was higher in the chamber. This illustrates that efficiency could be underestimated in the reactor regarding “real-world” applications. Further studies are needed to confirm these conclusions and it would be interesting to investigate light intensity of wavelengths exclusive to photo activity (use light filters for example). In any case, our results show that photocatalytic coatings applied to typical indoor material surfaces could be used to enhance indoor air quality regarding NO_x. In future studies, authors will use other pollutants (such as formaldehyde) and will try to upgrade experimental chamber equipment in order to measure eventual by-products and other gases who could interfere with the photocatalytic process (ozone for example).

4 CONCLUSIONS

Indoor air pollution poses serious treats to health comfort and productivity of occupants. Efficient techniques are required to reduce pollution and enhance air quality. Photocatalysis applied to indoor materials is a technique that has been widely studied and developed for this purpose. In this article, we have showed that NO₂ present indoors could be reduced with this technique. Laboratory results show a fair efficiency under typical indoor light. However, laboratory scale experimental apparatus might underestimate the photocatalytic activity. This type of test is not suitable for determining efficiency but is able to compare different parameters, such as light spectrum and intensity used for photo activation. Under “real-world” conditions, this technique seems to be quite effective in neutralising NO₂ even under visible light. Even though LED showed no activity, fluorescent and halogen light were well adapted. Further studies, using other light types, different pollution levels and other pollutants, are planned by the authors in the future.

ACKNOWLEDGEMENTS

The authors are grateful to CRISTAL for providing the photocatalytic products and to Bronkhorst for financing the equipment used for flow measurement and control.

REFERENCES

- [1] Maggos, T., Bartzis, J. G., Liakou, M. & Gobin, C., Photocatalytic degradation of NO_x gases using TiO₂-containing paint: A real scale study. *Journal of Hazardous Materials*, **146(3)**, pp. 668–673, 2007.

- [2] Maggos, T., Plassais, A., Bartzis, J. G., Vasilakos, C., Moussiopoulos, N. & Bonafous, L., Photocatalytic degradation of NO_x in a pilot street canyon configuration using TiO_2 -mortar panels. *Environmental Monitoring and Assessment*, **136(1–3)**, pp. 35–44, 2008.
- [3] Chen, J. & sun Poon, C., Photocatalytic construction and building materials: From fundamentals to applications. *Building and Environment*, **44(9)**, pp. 1899–1906, 2009.
- [4] Ohama, Y. & Van Gemert, D., *Applications of Titanium Dioxide Photocatalysis to Construction Materials*. Dordrecht: Springer Netherlands, 2011.
- [5] Horgnies, M., Dubois-Brugger, I. & Gartner, E. M., NO_x de-pollution by hardened concrete and the influence of activated charcoal additions. *Cement and Concrete Research*, **42(10)**, pp. 1348–1355, 2012.
- [6] Martinez, T., Bertron, A., Ringot, E. & Escadeillas, G., Degradation of NO using photocatalytic coatings applied to different substrates. *Building and Environment*, **46(9)**, pp. 1808–1816, 2011.
- [7] Ângelo, J., Andrade, L., Madeira, L. M. & Mendes, A., An overview of photocatalysis phenomena applied to NO_x abatement. *Journal of Environmental Management*, **129(x)**, pp. 522–539, 2013.
- [8] Boyjoo, Y., Sun, H., Liu, J., Pareek, V. K. & Wang, S., A review on photocatalysis for air treatment: From catalyst development to reactor design. *Chemical Engineering Journal*, **310**, pp. 537–559, 2017.
- [9] Ballari, M. M., Yu, Q. L. & Brouwers, H. J. H., Experimental study of the NO and NO_2 degradation by photocatalytically active concrete. *Catalysis Today*, **161(1)**, pp. 175–180, 2011.
- [10] Ballari, M. M. & Brouwers, H. J. H., Full scale demonstration of air-purifying pavement. *Journal of Hazardous Materials*, **254–255(1)**, pp. 406–414, 2013.
- [11] Folli, A., et al., Field study of air purifying paving elements containing TiO_2 . *Atmospheric Environment*, **107(2)**, pp. 44–51, 2015.
- [12] Guerrini, G. L., Photocatalytic performances in a city tunnel in Rome: NO_x monitoring results. *Construction and Building Materials*, **27(1)**, pp. 165–175, 2012.
- [13] Kleffmann, J., Discussion on ‘field study of air purification paving elements containing TiO_2 ’ by Folli et al. (2015). *Atmospheric Environment*, **129**, pp. 95–97, 2016.
- [14] Gallus, M., et al., Photocatalytic de-pollution in the Leopold II tunnel in Brussels: NO_x abatement results. *Building and Environment*, **84(2)**, pp. 125–133, 2015.
- [15] ISO 22197-1, Fine ceramics (advanced ceramics, advanced technical ceramics) - Test method for air-purification performance of semiconducting photocatalytic materials - Part 1: Removal of nitric oxide. *AFNOR*, 2016.
- [16] Ifang, S., Gallus, M., Liedtke, S., Kurtenbach, R., Wiesen, P. & Kleffmann, J. Standardization methods for testing photo-catalytic air remediation materials: Problems and solution. *Atmospheric Environment*, **91**, pp. 154–161, 2014.
- [17] Gallus, M., et al., Photocatalytic abatement results from a model street canyon. *Environmental Science and Pollution Research*, **22(22)**, pp. 18185–18196, 2015.
- [18] Hot, J., Martinez, T., Wayser, B., Ringot, E. & Bertron, A., Photocatalytic degradation of NO/NO_2 gas injected into a 10-m^3 experimental chamber. *Environmental Science and Pollution Research*, **24(14)**, pp. 12562–12570, 2017.
- [19] Topalov, J., Hot, J., Ringot, E. & Bertron, A., In situ NO abatement by photocatalysis—study under continuous NO injection in a 10-m^3 experimental chamber. *Air Quality Atmospheric Health*, **12(2)**, pp. 229–240, 2019.

- [20] Hot, J., Topalov, J., Ringot, E., & Bertron, A., Investigation on parameters affecting the effectiveness of photocatalytic functional coatings to degrade NO : TiO₂ amount on surface , illumination and substrate roughness. *International Journal of Photoenergy*, **2017**, pp. 1–14, 2017.
- [21] NF EN ISO 9972, Thermal performance of buildings - Determination of air permeability of buildings - Fan pressurization method, 2016.
- [22] Gaya, U. I. & Abdullah, A. H., Heterogeneous photocatalytic degradation of organic contaminants over titanium dioxide: A review of fundamentals, progress and problems. *Journal of Photochemistry and Photobiology C: Photochemistry Reviews*, **9(1)**, pp. 1–12, Mar. 2008.
- [23] Mamaghani, A. H., Haghghat, F. & Lee, C. S., Photocatalytic oxidation technology for indoor environment air purification: The state-of-the-art. *Applied Catalysis B: Environmental*, **203**, pp. 247–269, 2017.
- [24] Rajeshwar, K., Fundamentals of Semiconductors Electrochemistry and Photoelectrochemistry. *Encyclopedia Electrochemistry*, pp. 1–51, 2007.
- [25] Sivachandiran, L., Thevenet, F., Gravejat, P. & Rousseau, A., Investigation of NO and NO₂ adsorption mechanisms on TiO₂ at room temperature. *Applied Catalysis B: Environmental*, **142–143(2)**, pp. 196–204, 2013.
- [26] Horgnies, M., Dubois-Brugger, I. & Stora, E., An innovative de-polluting concrete doped with activated carbon to enhance air quality. in *10th International Concrete Sustainability Conference (NRMCA), At Miami (USA)*, 2015(July), pp. 0–13.
- [27] Hu, Y., Song, X., Jiang, S. & Wei, C., Enhanced photocatalytic activity of Pt-doped TiO₂ for NO_x oxidation both under UV and visible light irradiation: A synergistic effect of lattice Pt⁴⁺ and surface PtO. *Chemical Engineering Journal.*, **274(x)**, pp. 102–112, 2015.
- [28] Zhou, L., Tan, X., Zhao, L. & Sun, M., Photocatalytic oxidation of NO_x over visible-light-responsive nitrogen-doped TiO₂. *Korean Journal of Chemical Engineering*, **24(6)**, pp. 1017–1021, 2007.